ELSEVIER

Journal of Nuclear Materials 313–316 (2003) 153–157

journal of nuclear materials

www.elsevier.com/locate/jnucmat

Thermal annealing effects on chemical states of deuterium implanted into boron coating film

H. Kodama [a,*], T. Sugiyama [a], Y. Morimoto [a], Y. Oya [b], K. Okuno [c], N. Inoue [d], A. Sagara [d], N. Noda [d]

[a] *Graduate School of Science and Engineering, Shizuoka University, 836 Ohya, Shizuoka-shi, Shizuoka 422-8529, Japan*
[b] *Radioisotope Center, The University of Tokyo, 2-11-16 Yayoi, Bunkyo-ku, Tokyo 113-0032, Japan*
[c] *Radiochemistry Research Laboratory, Faculty of Science, Shizuoka University, 836 Ohya, Shizuoka-shi, Shizuoka 422-8529, Japan*
[d] *National Institute for Fusion Science, 322-6 Oroshi-cho, Toki-shi, Gifu 509-5292, Japan*

Abstract

To reveal interaction between boron coating film and energetic hydrogen isotopes, chemical states of deuterium implanted into the boron coating films deposited on graphite by using DC glow discharge in a diborane diluted helium have been studied. The XPS measurements showed the possibility of the formation of B–D and C–D bonds by D_2^+ ion implantation. The TDS experiments indicated that deuterium desorption took place in two stages, which were attributed to the desorption processes from the trapping sites of B–D and C–D bonds. The results of the XPS measurements after D_2^+ ion implantation revealed that the peak areas of the B–D and C–D bonds began to decrease at 310 and 473 K and the peaks almost disappeared at 873 and 1073 K, respectively. These results suggest that the trapping site of the B–D bond is largely influenced by thermal annealing effects compared with that of the C–D bond.

PACS: 52.40.Hf; 68.60.Dv
Keywords: Thermal annealing effect; Chemical state; Boronization; TDS; XPS

1. Introduction

For the purpose of impurity reduction in the plasma discharge, cleaning and gettering of impurities from plasma facing materials (PFMs) have been used in most fusion test devices [1,2]. In present, the major impurities in the vacuum vessels are thought to be carbon from carbon-based materials used as PFMs and oxygen. In order to suppress these impurities, conditioning procedures, such as boronization, have been applied to inner walls of the fusion devices. They led to remarkable improvements of operational performance in e.g. TEXOR, D-III, JT-60U, and so on [3–6]. The effects of boronization on the interaction between boron coating films and the impurities, in particular oxygen, also have been reported [7,8].

During the plasma operation, PFMs are exposed not only to the fast neutron but also to energetic particles, such as tritium, deuterium, and helium. From the viewpoint of safety for D–T fusion reactors, it is required to study tritium behavior and estimate tritium inventory in PFMs. In fusion reactors performing boronization, it is, in particular, necessary that tritium behavior and tritium inventory in boron coating films are elucidated.

In the present study, the chemical states of deuterium implanted into boron coating film and the depth profiles of the constituent atoms of the boron coating film were studied by means of X-ray photoelectron spectroscopy (XPS) and thermal desorption spectroscopy (TDS). For the purpose of making clear the correlation between the chemical states and the desorption behavior of the

* Corresponding author. Tel.: +81-54 238 6436; fax: +81-54 238 3989.
E-mail address: r0132004@ipc.shizuoka.ac.jp (H. Kodama).

0022-3115/03/$ - see front matter
PII: S0022-3115(02)01404-6

implanted deuterium, their thermal annealing effects on chemical states of implanted deuterium were also investigated by the combination of XPS and TDS.

2. Experimental

2.1. Sample preparation and characterization

Sample preparation was performed in a plasma processing test stand device at the National Institute for Fusion Science (NIFS) [9]. Boron coating was deposited by DC glow discharge ($P = 100$ W) in a mixture of diborane (vol. 3%) and helium (vol. 97%). The boron coating films were deposited on the isotropic graphite substrates (size: $10^{\phi} \times 1.0^{t}$ mm, density: 1.83 g cm^{-3} (IG-430U: Toyotanso Co. Ltd.)), used as the PFMs in the large helical devices (LHD) at NIFS. The thickness of the deposited films was determined by a quartz oscillator to be 200 nm.

The depth profiles of the film constituents (B, C, N, and O) in the boron coating film were analyzed by XPS (ESCA 1600, ULVAC-PHI Inc.) with 2.0 keV Ar^+ ion beam sputtering. The XPS apparatus was described in our previous paper [10].

Fig. 1 shows the depth profiles of elements in the film. The atomic ratios of boron and carbon within the film were almost constant (B/C = 2.6) between 2.0×10^{20} and 1.3×10^{21} Ar^+ m^{-2}. Oxygen and nitrogen distributed uniformly and their composition ratios decayed gradually with a constant rate.

2.2. Chemical states of implanted deuterium

The chemical states of the deuterium implanted into the boron coating film were evaluated by XPS. As shown in Fig. 1, boron and carbon were the major elements in the boron coating film. The 1.0 keV D_2^+ ions were implanted into the sample with the flux of 1.0×10^{18} D^+ m^{-2} s^{-1} and the fluence of 1.5×10^{22} D^+ m^{-2}. The implantation area was 3.0×3.0 mm^2 at the angle of incidence of 0° to the surface normal, and the sample was kept at 303 K. The chemical states of B-1s and C-1s in the boron coating film were analyzed by XPS before and after the D_2^+ ion implantation. The D_2^+ ion implantation and XPS measurements were repeated sequentially in situ until the deuterium fluence reached 1.5×10^{22} D^+ m^{-2}.

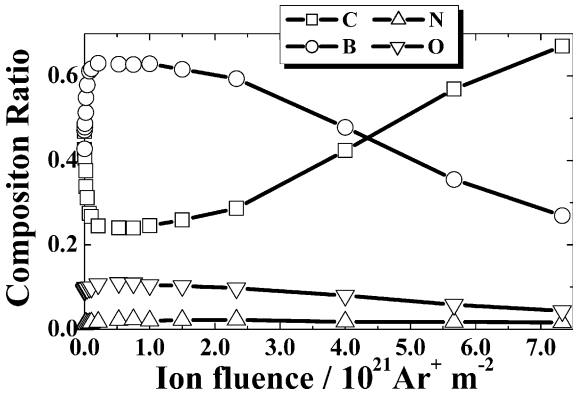

Fig. 1. The depth profile of atomic composition ratio in boron coating film by XPS using Ar^+ ion sputtering.

In order to elucidate deuterium desorption behaviors, the deuterium ions were implanted into the boron coating film with the fluence of 1.0×10^{22} D^+ m^{-2}. The deuterium ion implantation conditions were the same as those of the above XPS experiment. After the D_2^+ ion implantation, the sample was heated from 303 to 1353 K at a heating rate of 0.5 K s^{-1}. The released gases were measured by a quadrupole mass spectrometer (QMS). Our TDS experimental setup was also described in Ref. [10].

2.3. Thermal annealing effects on chemical states of implanted deuterium

After the D_2^+ ion implantation, the thermal annealing experiments for the samples were performed at each temperature, 473, 573, 723, 873, 1073, and 1353 K for 1 min. The conditions of D_2^+ ion implantation and the annealing rate were the same as those in the TDS experiment. After heating up to each temperature with the heating rate of 0.5 K s^{-1}, the sample was cooled down to room temperature and the chemical states of B-1s and C-1s were evaluated in situ by XPS.

3. Results

Fig. 2 shows the dependence of the peak top binding energy of the B-1s peak of the XPS signal as a function of the deuterium ion fluence. The peak top energy of the B-1s peak was shifted to the high energy side at the fluence less than 5.0×10^{21} D^+ m^{-2}, and remained fairly constant above 5.0×10^{21} D^+ m^{-2}.

Fig. 3 shows the analyzed results of the B-1s and C-1s peaks. The B-1s peak was divided into five peaks, of which each binding energy was taken from the literature's values [7,8,11–14]. The interaction between carbon, a second major constituent element in the boron coating film, and the implanted deuterium also should be considered. The C-1s peak in the XPS spectrum was also divided into four peaks as shown in Fig. 3 [8,11,12,14]. The peaks of the C–B bond and B–C–B bond were separately indicated in this figure. As the amount of boron was about 2.5 times as large as that of carbon in the boron coating film, the B–C–B bond means boron rich bond, where the carbon attracts more electron from the surrounding borons than that of C–B

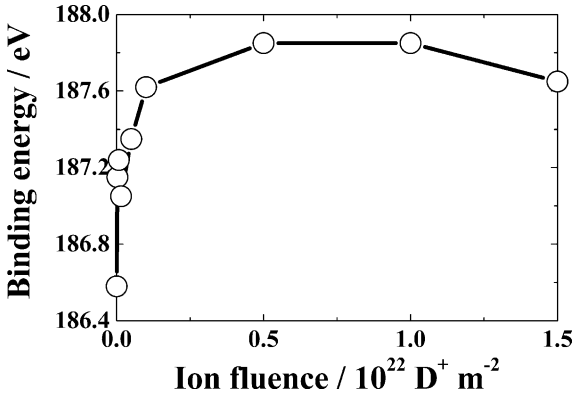

Fig. 2. The dependence of B-1s peak top binding energy on deuterium ion fluence.

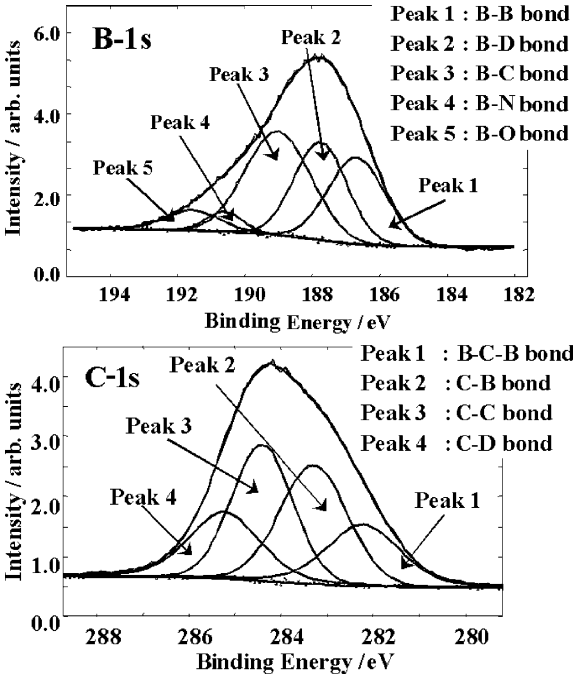

Fig. 3. The analyzed XPS spectra of B-1s and C-1s after D_2^+ ion implantation.

bond, due to its higher electronegativity. The higher electron density on the carbon of B–C–B bond could result in shift to lower binding side than that of C–B bond.

Fig. 4 shows the TDS spectrum of D_2 released from the boron coating film after D_2^+ ion implantation. The D_2 gas was released in the temperature region from 300 to 1150 K. As a shoulder was observed at around 600 K in the TDS spectrum of the D_2 release, the TDS peak was divided into two peaks (peak 1 around 500 K and peak 2 around 800 K) using a Gaussian distribution function. The released amount of the D_2 at peak 2 was approximately 2.5 times larger than that at peak 1.

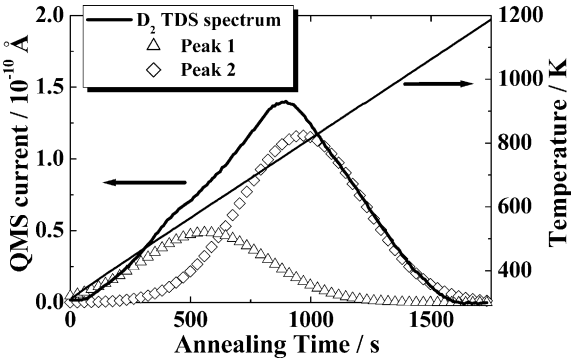

Fig. 4. The analyzed TDS spectrum of D_2 released from boron coating film after D_2^+ ion implantation.

Fig. 5 shows the correlation between the peak 1 and 2 of the TDS spectrum and the XPS peak areas of the B–D and C–D bonds. The peak areas of the B–D and C–D bonds began to decrease around 310 and 473 K and almost disappeared around 873 and 1073 K, respectively. This suggests that the dissociation temperature regions of the B–D and C–D bonds differ. On the other hand, the temperature region of the deuterium desorbed by thermal annealing was from about 300 to 900 K for peak 1 and from 450 to 1100 K for peak 2. The temperature regions of peaks 1 and 2 in the TDS spectrum corresponded to those for the decreasing of the peak areas of the B–D and C–D bonds, respectively. This shows that there is the close correlation between the XPS and TDS results after the D_2^+ ion implantation.

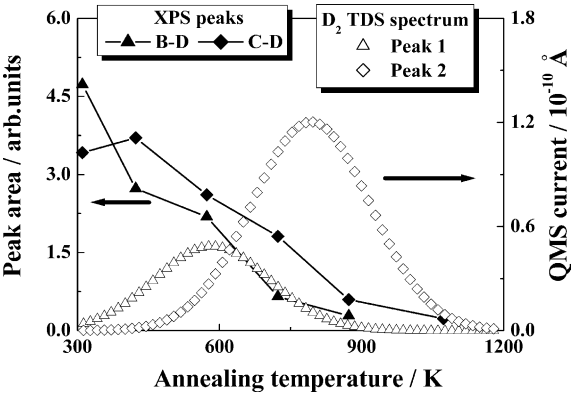

Fig. 5. The comparison between the peak 1 and 2 of the TDS spectrum and the peak areas of B–D and C–D bonds of the XPS.

4. Discussion

In the B-1s peak of the XPS spectrum, the chemical shift to the high binding energy side was induced by reduction of electron density on boron, which was caused by deuterium attracting the valence electrons of boron due to its stronger electronegativity than that of boron [11]. In the other words, the chemical shift was attributed to the formation of the B–D bond. In the C-1s peak of the XPS spectrum, the chemical shift to the high binding energy side attributed to the formation of the C–D bond by D_2^+ ion implantation. The region of deuterium ion fluence more than 5.0×10^{21} D m^{-2}, in which the peak top energy of the B-1s and C-1s peaks was constant, corresponded to that, in which the peak area of the B–D and C–D bonds were constant. These arose from the equilibrium between the formation of the B–D and C–D bonds, and disordering of the initial structure in the boron coating film. These results indicated that the deuterium implanted into the boron coating film was trapped by two trapping sites, namely B–D and C–D bonds.

From analyzing the TDS spectrum as shown in Fig. 4, it suggested that two trapping sites for the implanted deuterium existed in the boron coating film. The TDS spectrum of the boron coating film was similar to that of B_4C and boron–carbon film with H^+ and D^+ implantation, respectively [15,16]. It was reported that the H_2 release from B_4C was ascribed to the detrapping of hydrogen from C–B and C–H bonds. It was also reported that the D_2 release from boron–carbon films was attributed to the detrapping from the B–D and C–D bond. In the both cases, the release temperature of H_2 or D_2 from the boron trapping site was lower than that from the carbon trapping site. Taking into account these, it is suggested that peak 1 and 2 shown in Fig. 4 result from deuterium detrapping from the B–D and C–D bond in the boron coating film, respectively.

As shown in Fig. 5, the temperature regions of peak 1 and 2 corresponded to those for the decrease and disappearance of the XPS peak of the B–D and C–D bonds, respectively. The C–D bond existed at the temperatures of over 873 K, where the B–D bond had already disappeared. These suggest that the implanted deuterium interacts more strongly with carbon than boron. In fact, the activation energy of the H_2 desorption from the C–H bond (1.7 ± 0.3 eV) in B_4C was reported to be bigger than that from the B–H bond (1.2 ± 0.4 eV) [15].

Although the concentration ratio of carbon to boron was 0.38, the D_2 release from the C–D bond, peak 2, was approximately 2.5 times as large as that from the B–D bond, peak 1. This shows that carbon plays a more effective role in trapping the implanted deuterium than boron. Therefore, if pure boron coating film were prepared in the boronization of fusion reactors, the tritium inventory should be minimized.

5. Conclusion

The annealing effects on the chemical states of deuterium implanted into the boron coating film, which was prepared by DC glow discharge using a mixture of diborane and helium gases, were investigated by means of XPS and TDS.

Observations were made of the chemical shifts of B-1s and C-1s peaks by XPS and of the two desorption processes by TDS. The results of TDS and XPS experiments suggest that deuterium implanted into our prepared boron coating film is trapped to both boron and carbon by forming the B–D and C–D bonds.

The experimental results of XPS and TDS for the D_2^+ ion implanted sample after the thermal annealing at different temperature are as follows: The XPS peak area of the B–D bond decreased in the temperature region from 310 to 873 K, which is consistent with the region of D_2 desorption of the first TDS peak. The temperature region for decrease of the C–D bond peak from XPS corresponds to that of peak 2 from TDS. The annealing experiments also suggested that the trapping site of the B–D bond is more easily influenced by thermal annealing effects than is the C–D bond. In the present study, the correlation between the chemical states and the desorption behavior of the deuterium implanted into the boron coating film was elucidated.

Acknowledgement

This study was performed with the support and under the auspices of the NIFS Collaborative Research Program.

References

[1] G.L. Jackson, T.S. Taylor, P.L. Taylor, Nucl. Fusion 30 (1990) 2305.
[2] J. Winter, J. Nucl. Mater. 176&177 (1990) 14.
[3] H. Toyoda, H. Ninomiya, T. Isozumi, T. Okada, Appl. Phys. Lett. 51 (1987) 798.
[4] J. Winter et al., J. Nucl. Mater. 162–164 (1989) 713.
[5] M.M. Ennaceur, B. Terreault, J. Nucl. Mater. 280 (2000) 33.
[6] R. Zehringer, H. Künzli, P. Oelhafen, C. Hollenstein, J. Nucl. Mater. 176&177 (1990) 14.
[7] G.L. Jackson et al., J. Nucl. Mater. 196–198 (1992) 236.
[8] M. Saidoh et al., Jpn. J. Appl. Phys. 32 (1993) 3276.

[9] M. Natsir, A. Sagara, O. Motojima, J. Nucl. Mater. 220–222 (1995) 865.
[10] Y. Morimoto, T. Sugiyama, S. Akahori, H. Kodama, E. Tega, M. Sasaki, M. Oyaidu, H. Kimura, K. Okuno, Phys. Scr., in press.
[11] H.O. Pitchard, H.A. Skinner, Chem. Rev. 55 (1955) 745.
[12] M. Dinescu, A. Perrone, A.P. Caricato, L. Mirenghi, C. Gerardi, C. Ghica, L. Frunza, Appl. Surf. Sci. 127–129 (1998) 692.
[13] D.J. Joyner, D.M. Hercules, J. Chem. Phys. 72 (2) (1980) 1095.
[14] J. Von Seggern, P. Wienhold, H.G. Esser, J. Winter, A. Gorodesky, S. Grashin, I. Gudowska, G.G. Ross, J. Nucl. Mater. 176&177 (1990) 357.
[15] Y. Yamauchi, Y. Hirohata, T. Hino, T. Yamashima, T. Ando, M. Akiba, J. Nucl. Mater. 220–222 (1995) 851.
[16] T. Yamaki, Y. Gotoh, T. Ando, R. Jimbou, N. Ogiwara, M. Saidoh, J. Nucl. Mater. 217 (1994) 154.